Spatial Measurement Quality of Ground-Based Weather Radar Using Surrounding Terrain with Open-Source Radar Library

Nattapon Mahavik[1,5*], Fatah Masthawee[1,2], Sarawut Arthayakun[1,3], Apichaya Kangerd[1], Jamorn kunwilai[1], Wirachart Promta[2], Chanin Umponstira[1], Charatdao Kongmuang[1,5], Sarintip Tantanee[4,5]

[1]Department of Natural Resources and Environment, Faculty of Agriculture Natural Resources and Environment, Naresuan University, Phitsanulok 65000 Thailand
[2]Thai Meteorological Department, Bangkok 10260 Thailand
[3]Department of Royal Rainmaking and Agricultural Aviation, Bangkok, 10900 Thailand
[4]Department of Civil Engineering, Faculty of Engineering, Naresuan University, Phitsanulok 65000 Thailand
[5]Water Resources Research Center, Faculty of Engineering, Naresuan University, Phitsanulok 65000 Thailand
*Email : nattaponm@nu.ac.th

Abstract: *This work provides a comprehensive examination of Partial Beam Blockage (PBB) and Cumulative Beam Blockage (CBB) seen in the Chiang Rai radar located in northern Thailand. The main objective is to investigate the influence of complex terrain on the propagation of radar beams. Quantitative analysis of beam obstruction in different azimuthal directions shows substantial blockage (CBB > 0.8) in the western and northwestern sectors caused by hilly terrain, whereas little blockage (CBB < 0.2) is seen in the eastern and southeastern sections. This study employed the wradlib software to interpolate CBB data from polar to geographic coordinates using both linear and closest neighbor techniques. Linear interpolation yielded a more seamless spatial continuity, but nearest neighbor interpolation maintained the original data values with more precision. The data were displayed in QGIS, visualizing the patterns of beam blockage overlaid on a topographic base map to emphasize the relationships between blockage and terrain characteristics. The investigation was expanded to include various elevation angles, revealing that at higher angles (1.5 degrees), the obstruction in the eastern and southern sectors diminished, thereby enhancing radar coverage in those specific directions. This increased visibility has significant consequences for meteorological monitoring, particularly in the identification of tropical cyclones and thunderstorms, as well as for aviation surveillance. Integration of CBB data into GIS enables sophisticated spatial analysis, facilitating improved optimization of radar networks for organizations such as the Thai Meteorological Department (TMD). The present work enhances an understanding of radar beam propagation in mountainous areas and provides valuable insights for enhancing radar operations and data interpretation in challenging environments.*

Keywords: Partial Beam Blockage, Thailand, Topography impact, Radar meteorology, GIS

1. Introduction

Weather radar systems are crucial for meteorological observations, as they provide vital data for weather prediction, storm monitoring, and climate research. Nevertheless, both the accuracy and reliability of radar measurements can be greatly affected by partial beam blockage (PBB), especially in areas with intricate topography (Bech et al., 2003). Recent research has emphasized the ongoing difficulties that PBB presents to radar meteorology.

McKee and Binns (2016) have shown how PBB affects the accuracy of estimating precipitation in areas with mountains. The Chiang Rai weather radar, located in the mountainous region of northern Thailand, serves as a prime example of these difficulties. This work aims to precisely evaluate and reduce the impact of PBB on the quality of radar data in complicated environments. This research combines high-resolution digital elevation models (DEMs) with advanced radar simulation techniques to replicate PBB using the methodology presented by Zhang et al. (2013) and the more recent developments by Gou & Chen (2020). The simulation is based on the work of Bech et al. (2003).

The progress made in open-source radar software has greatly improved the capacity to simulate and evaluate weather radar data in complex landscapes. Wradlib, a Python library for analyzing weather radar data, demonstrates the advancements made in this field (Heistermann et al., 2013). Researchers can use it to model the propagation of beams and their interaction with digital elevation models (DEMs), which allows for a better understanding of radar performance in different topographies. In hilly terrain, radar observations are frequently affected by ground clutter and beam blockage, which have a significant impact on the quality and interpretation of the data (Friedrich et al., 2016). The capabilities of Wradlib have been explored in recent research projects using polarimetric radar data collected from the Chiang Rai station located in northern Thailand (Mahavik et al., 2023, 2024). These studies demonstrate the effective application of open-source tools in real-world situations, promoting collaboration among scientists. By utilizing these libraries, researchers can enhance their ability to measure and reduce the impact of beam blockage, hence enhancing the reliability of weather radar data in areas with complex terrain. This technological progress improves our capacity to examine extreme weather phenomena and supports to more accurate forecasting and enhanced resilience for disasters in mountainous regions.

The benefits of PBB extend beyond fundamental weather observations, impacting many applications of radar data. Precise radar coverage is essential in aviation for ensuring flight safety and optimizing air traffic management, as highlighted in recent research by Saltikoff et al. (2018) regarding the use of weather radar in aviation meteorology. PBB, or precipitation bias correction, can cause substantial inaccuracies in rainfall estimation, which can have a negative effect on flood forecasting and the management of water resources (Speirs et al., 2017). This study enhances the existing knowledge by creating a thorough technique for PBB analysis, which incorporates polar-to-Cartesian data interpolation, integration with Geographic Information System (GIS), and multi-angle beam propagation modeling.

The study utilizes the latest developments in radar meteorology and precipitation analysis, as indicated by Dai et al. (2019), who employed advanced modeling approaches and dual-polarization radar to address differences between radar and gauge rainfall measurements. In addition, the study overcomes the limitations identified in previous research on beam blockage by offering an accurate representation of the spatial variations in radar coverage. This aligns with the recent efforts made by He et al. (2018) to enhance the quality control of radar data in areas with complex terrain. Another aim is to exhibit the practical utility of this PBB analysis in enhancing radar operations and enhancing data interpretation for

meteorological operation. This is consistent with recent initiatives by national meteorological services to improve the effectiveness of radar networks, as described by Saltikoff et al. (2019) in their investigation of the latest weather radar capabilities.

Therefore, this work aims to create and apply a reliable approach for analysing PBB under the geographical constraints. This task involves investigating the arrangement of obstacles that blocks the path of a radar beam at various angles of elevation. It also requires assessing the impact of these obstructions on the accuracy of radar data and meteorological observations in the Chiang Rai area. The results have important consequences for improving the efficiency of weather radar networks, especially for organizations such as the Thai Meteorological Department (TMD) that operate and utilize these systems in various parts of the country.

2. Study area

The focus of this research is the weather radar station situated in Chiang Rai province locates in northern Thailand, as depicted in Figure 1. The radar location locates in the geographical coordinates of 99.881618°E longitude and 19.961643°N latitude, with an elevation of 387 meters above sea level. The height was calculated using SRTM3Arc (Shuttle Radar Topography Mission 3 arc-second) data, which offers a detailed digital elevation model (DEM) of the surrounding topography.

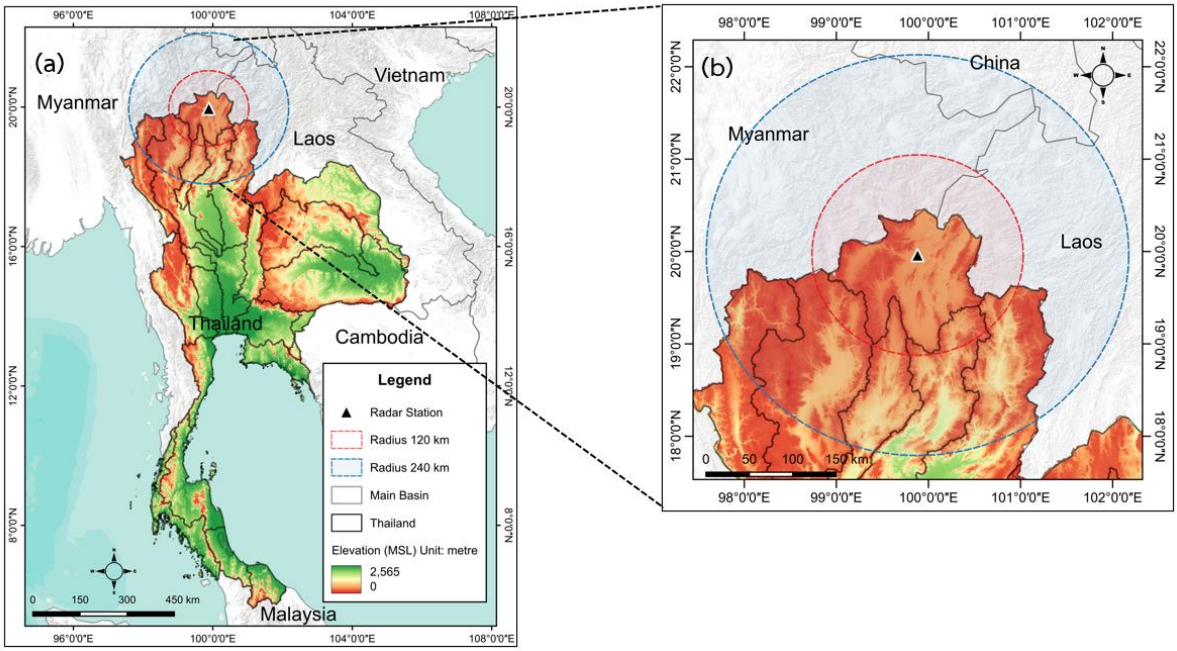

Figure 1: Study area for analyzing the quality of radar measurements using beam propagation simulation for the Chiang Rai radar, northern Thailand (a) Thailand (b) radar observation areas for red and blue lines indicate 120 and 240 km radius, respectively.

The landscape of Chiang Rai is characterized by mountainous regions, valleys, and plains, which makes it a perfect site for investigating the impact of PBB on weather radar measurements. The radar has a maximum range of 240 kilometers and covers a wide area that includes parts of the Golden Triangle region where Thailand, Laos, and Myanmar connect. The radar observation area encompasses two mountain ranges, namely Daen Lao and Phi Pan Nam, located in the northernmost and western regions, respectively. Furthermore, there are two primary rivers, namely the Kok and Ing rivers, which flow in an easterly direction to converge with the Mekong River.

In this investigation, we particullary concentrated on an azimuth angle, utilizing a radar system that was set up to employ 360 rays and 480 range bins. The range resolution was configured to 500 meters, enabling detailed examination of beam blockage effects at different distances from the radar location. The elevation angle of 1.0 degree was selected to investigate air conditions at low altitudes, where the obstruction of the radar beam by terrain interference can be most noticeable.

This study area provide a valuable chance to adapt and evaluate techniques for measuring PBB in complex landscapes, which can enhance accuracy of radar and meteorological observations over mountainous regions.

3. Data and Methodology

3.1 Data Sources

This study utilizes a combination of weather radar data and DEM information to analyze PBB. The primary data sources are as follows:

Weather Radar Data: The analysis is based on data from the weather radar station in Chiang Rai, Thailand (99.881618°E, 19.961643°N, elevation 387m). TMD operates a C-band radar to observe weather conditions within a radius of 240 km in the eastern part of northern Thailand. There are four elevation angles observed every 15 minutes (Mahavik et al. 2024; Mahavik et al. 2023). The radar parameters include:

- Number of rays: 360
- Number of range bins: 480
- Range resolution: 500 meters
- Half-power beam width: 1.0 degree
- Elevation angle: 1.0 degree

These specifications allow for a detailed examination of the radar's coverage area, extending to a maximum range of 240 km.

DEM: Terrain data is sourced from the Shuttle Radar Topography Mission 3 arc-second (SRTM3Arc) dataset. This high-resolution DEM provides accurate elevation information for the study area. The data is stored in a GeoTIFF format and is processed using the wradlib library in Python.

Software and Libraries: The analysis is conducted using Python, with the Wradlib library (Heistermann et al. 2013) playing a crucial role in processing both radar and DEM data. Additional Python libraries utilized include matplotlib for visualization, numpy for numerical computations, and gdal (accessed through wradlib) for handling geospatial data.

These data sources and tools enable a comprehensive analysis of partial beam blockage, combining precise radar measurements with detailed terrain information to improve the accuracy of weather radar observations in complex topography.

3.2 Methodology

The assessment of PBB in this study employs an approach that combines high-resolution DEM data with radar beam propagation models, as depicted in Figure 2. The code we have created is available at the following link: https://github.com/nattaponm/Beam_blockage_radar_Thai. The methodology utilizes the wradlib library, which is a specific Python package designed for the processing and analysis of weather radar data. The investigation of PBB starts by collecting and preparing SRTM DEM 3 arc-second data that covers the radar station region. The Digital Elevation Model (DEM) is subsequently processed to be aligned with the coordinate system of the radar and clipped to fit inside of the radar's coverage area. The preprocessed digital elevation model (DEM) is imported into the Wradlib Python library (Heistermann et al., 2013), which is set up with specific radar settings such as location, elevation, and beam characteristics. The radar beam propagation is simulated using Wradlib functions, which calculate the height and breadth of the beam at each range bin. The analysis primarily consists of calculating the PBB and cumulative beam blockage (CBB) along each radar ray using the specific functions provided by Wradlib. In order to visually examine and study the outcomes, PPI (Plan Position Indicator) plots are created for both the elevation of the terrain and CBB, in addition to beam profile plots for certain azimuths to demonstrate the patterns of blockage. Finally, the polar CBB data is converted into a Cartesian grid and saved as a georeferenced TIFF file, allowing for easier investigation in GIS applications. This methodology integrates detailed terrain data with advanced radar modeling techniques, offering an effective way to measure beam blockage and enhance the quality of radar data in intricate topography conditions.

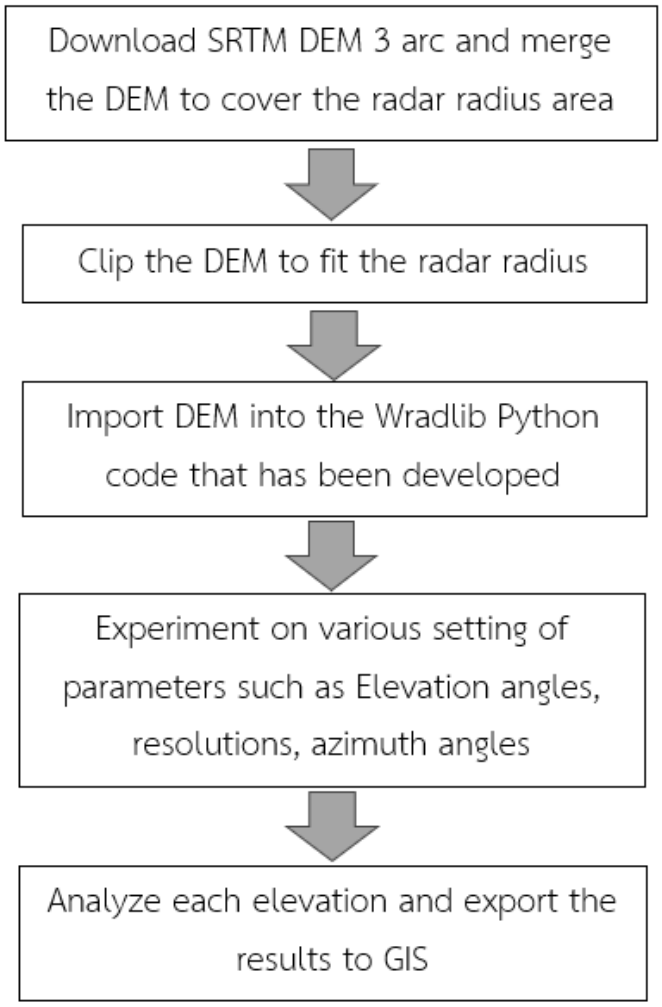

Figure 2: Workflow for analyzing the quality of the Chiang Rai ground-based weather radar using surrounding terrain. This workflow illustrates the process of simulating beam interaction with DEM using Wradlib and GIS

3.2.1 PBB Calculation Method

The PBB is quantified using the beam blockage fraction (BBF) method (Bech et al., 2003), which calculates the proportion of the radar beam cross-section obstructed by terrain. The BBF at a given point along the radar beam path is expressed as:

$$BBF = A_{blocked} / A_{total} \quad \ldots \text{Equation (1)}$$

where A_blocked is the area of the beam cross-section blocked by terrain, and A_total is the total area of the beam cross-section.

The cumulative beam blockage fraction (CBB) at range r is then calculated as:

CBB(r) = 1 - product(1 - BBF_i) …..Equation (2)

where BBF_i is the beam blockage fraction at each range bin up to r, and the product is taken from i=1 to r.

3.2.2 DEM Integration

The DEM data is integrated into the PBB calculations through the following steps:

1. Coordinate transformation: The DEM data is reprojected to match the radar coordinate system using wradlib.georef.reproject_raster_dataset.

2. Beam path modeling: The radar beam path is modeled considering the Earth's curvature and atmospheric refraction, using the equivalent Earth radius model (Delrieu et al. 1995):

h(r) = sqrt(r^2 + (k_e * R_e)^2 + 2r * k_e * R_e * sin(theta)) - k_e * R_e + h_0 …Equation (3)

where h(r) is the beam height at range r, k_e is the effective Earth radius factor (typically 4/3), R_e is the Earth's radius, theta is the elevation angle, and h_0 is the radar antenna height.

3. Terrain intersection: The beam height is compared with the DEM elevation at each point along the beam path to determine blockage.

3.2.3 Software and Tools

The study is predominantly performed using Python, utilizing multiple essential modules for various areas of data processing and display. Wradlib is used for performing calculations and creating visual representations particular to radar data, while numpy is used for carrying out numerical computations. Matplotlib is the main tool used for plotting and visualization activities. QGIS is utilized for spatial data modification and visualization when there is a need for further GIS processing. Python has been used to perform analysis within the defined workflow.

4. Results

4.1 Partial Beam Blockage analysis

The investigation of PBB for the Chiang Rai radar demonstrates notable differences in beam obstruction across various azimuthal directions, as depicted in Figure 3. Figure 3a exhibits a topographic map of the area, depicting altitudes ranging from sea level (blue) to almost 2000 meters (brown). The complex topography has a direct impact on the way the radar beam path, as can be shown in Figure 3b illustrating the distribution of CBB. The CBB map shows significant obstruction (shown by dark red color, CBB > 0.8) in many sectors, namely in the

western and northwestern quadrants. This obstruction is probably caused by the presence of elevated land features in these directions. In contrast, the eastern and southeastern sectors exhibit insignificant blockage (shown by white to light pink color, CBB < 0.2), which corresponds to the lower altitude regions seen in the topographic map. The beam profile plot in the lower panel presents an accurate measurement of the blockage area along a particular azimuth (60 degrees, as denoted by the red line in the Figure 3a). Figure 3c illustrates the interaction between the beam and the terrain. The ground elevation is depicted by the grey area, while the beam center and 3dB bounds are represented by the blue lines. Terrain obstructs the radar viewing area in the west and northwest regions. The northern part is connected to the Daen Lao mountain range, while the western area is encompassed by the Phi Pan Nam mountain range.

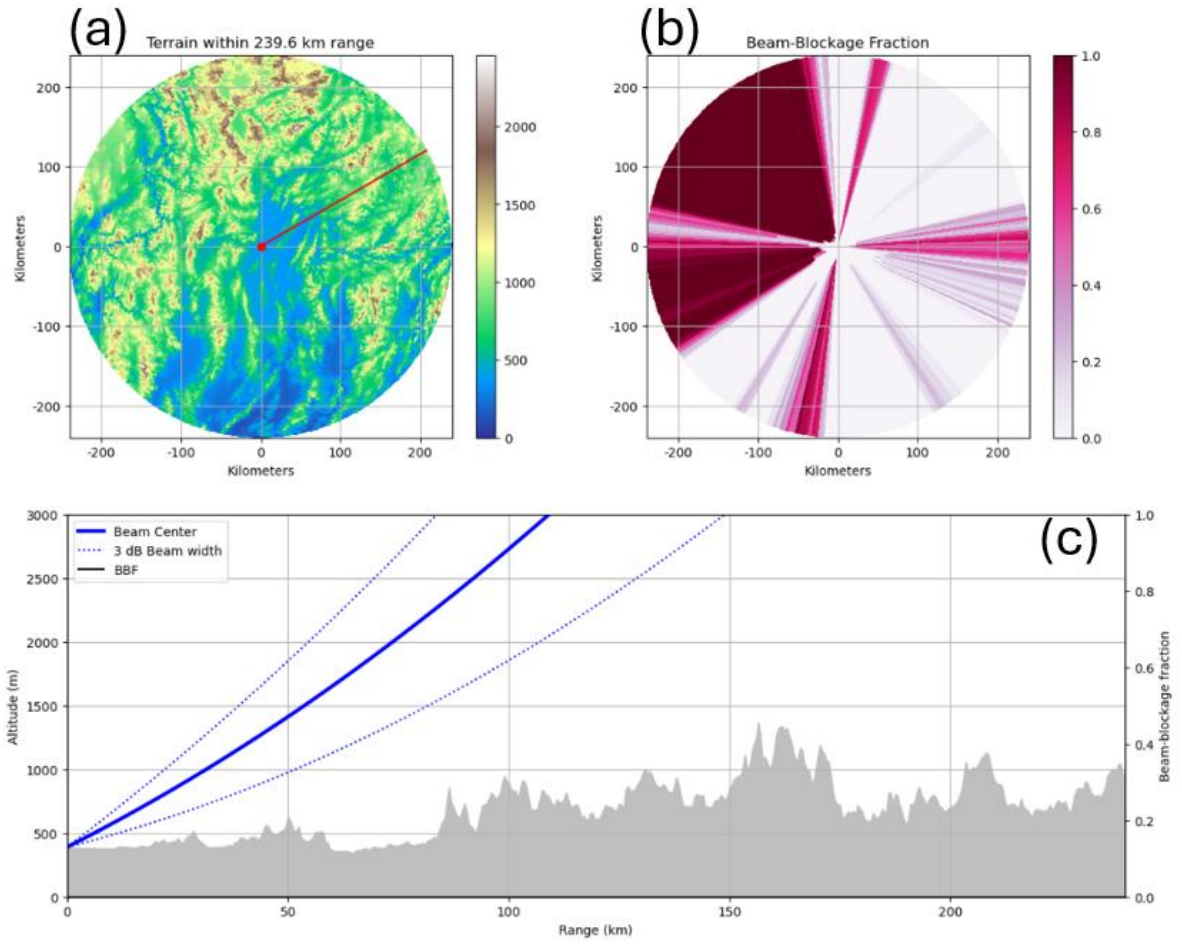

Figure 3: Results of beam simulation interacting with DEM for the first elevation angle of 1.0 degree

4.2 Cumulative Beam Blockage in Geographic coordinates

The interpolation process transforms CBB data from its original polar coordinate system to a geographic grid-based system, facilitating easier integration with other geospatial data. This transformation involves interpolating the CBB values from their source data in polar coordinates to a defined target grid in latitude-longitude coordinates. To accomplish this, we

employ two interpolation methods provided by the wradlib library: linear and nearest neighbor interpolation as shown in Figure 4.

```
import wradlib.ipol as ipol
from wradlib.vis import plot_ppi
src = polcoords
vals = CBB
src = np.reshape(src,[360*480,2])
vals = np.reshape(vals,[360*480])
xtrg = np.linspace(src[:, 0].min(), src[:, 0].max(), 400)
ytrg = np.linspace(src[:, 1].min(), src[:, 1].max(), 400)
trg = np.meshgrid(xtrg, ytrg)
trg = np.vstack((trg[0].ravel(), trg[1].ravel())).T
ip_lin = ipol.Linear(src, trg)
result_lin = ip_lin(vals.ravel(), fill_value=np.nan)
ip_near = ipol.Nearest(src, trg)
maxdist = trg[1, 0] - trg[0, 0]
result_near = ip_near(vals.ravel(), maxdist=maxdist*2)
```

Figure 4: Code excerpt for interpolating CBB from polar coordinates to a geographic Cartesian grid

The method begins by transforming the original coordinates (polcoords) and CBB values into arrays with a single dimension, making them suitable for the interpolation functions, as depicted in Figure 5. The target grid is defined by generating equidistant points along the x and y axes, with the grid extent determined by the minimum and maximum values of the source data. The grid is created using numpy's linspace and meshgrid functions to ensure comprehensive coverage of the geographical area of the original data. To do linear interpolation, the ipol.Linear function from the wradlib library has been applied. This method computes CBB values for every point in the target grid by using a linear combination of the closest source points. On the other hand, the nearest neighbor interpolation, which is carried out using the ipol.Nearest method, assigns the CBB value from the closest source point to each destination grid point. This method maintains the original data values with greater precision, but it may lead to a less visually smooth look, particularly in regions with abrupt changes. The maxdist value, an essential parameter in nearest neighbor interpolation, is defined as twice the distance between neighboring grid points. This interpolation takes into account an adequate radius around each target point to balance between data coverage and computational performance. The interpolated data sets yield two distinct representations of the CBB information in a standardized geographic grid. Figure 5 illustrate the transformation of the original polar coordinate data (Figure 5a) into two Cartesian representations: one utilizing linear interpolation (Figure 5b) and the other utilizing nearest neighbor interpolation (Figure 5c). These gridded datasets allow for more convenient comparison with other geographic data layers and provide additional spatial study of beam blockage patterns.

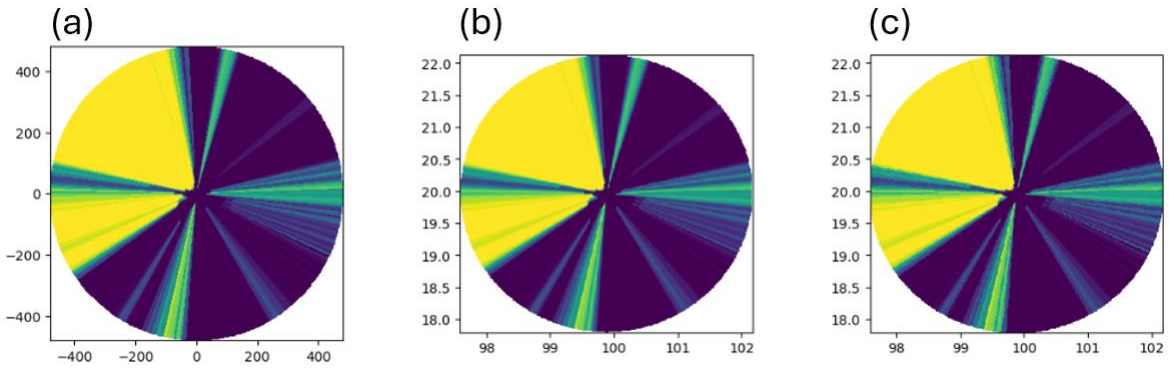

Figure 5: Results of CBB displayed in Matplotlib: (a) CBB plotted in polar coordinates; (b) CBB interpolated from polar to Cartesian grid of geographic coordinates using linear interpolation; (c) same as middle but using nearest neighbor interpolation

The integration of CBB data into GIS significantly enhances the ability to manipulate and analyze this crucial meteorological information. To facilitate this integration, we employ wradlib functions to export our interpolated CBB data, which is in a Cartesian grid of geographic coordinates, to a GIS-compatible format. The process begins by reshaping the interpolated CBB data into a 400x400 grid structure (CBB_grid), ensuring it aligns with our predefined geographic extent. Concurrently, we reshape the target grid coordinates (trg) into a matching 400x400x2 array (trg_grd), preserving the spatial reference information.

Using wradlib's georef.raster.create_raster_dataset function, we combine the CBB_grid data with the trg_grd coordinate information to create a georeferenced raster dataset (CBB_rt). This crucial step embeds the geographic coordinate system into the data structure. Finally, we utilize the wrl.io.write_raster_dataset function to export this dataset as a GeoTIFF, a format widely supported in GIS applications.

```
CBB_grid=np.reshape(result_near, (400,400))
trg_grd=np.reshape(trg,(400,400,2))
CBB_rt=wrl.georef.raster.create_raster_dataset(CBB_grid,trg_grd)
wrl.io.write_raster_dataset("CBB_cri_geotif.tif", CBB_rt, "GTiff")
```

Figure 6: Excerpt of Python code to export CBB in geographic coordinates to GeoTIFF format for use in GIS

4.3 Visualization CBB in GIS

The resulting GeoTIFF file is subsequently loaded into QGIS, a robust open-source GIS software. As demonstrated by the QGIS snapshot presented in Figure 7, the CBB data is accurately superimposed on a base map, most likely Google Maps or a comparable service. The radar's coverage area is readily visible in a circular pattern, with different colors indicating varying levels of beam blockage. The integration with QGIS facilitates accurate spatial alignment, enabling us to establish correlations between beam blocking patterns and

topographical characteristics, urban regions, and other geographical elements. This visualization can confirm the accuracy of our data processing and export operations, while also offer useful insights into the spatial distribution of radar beam blockage in the Chiang Rai region.

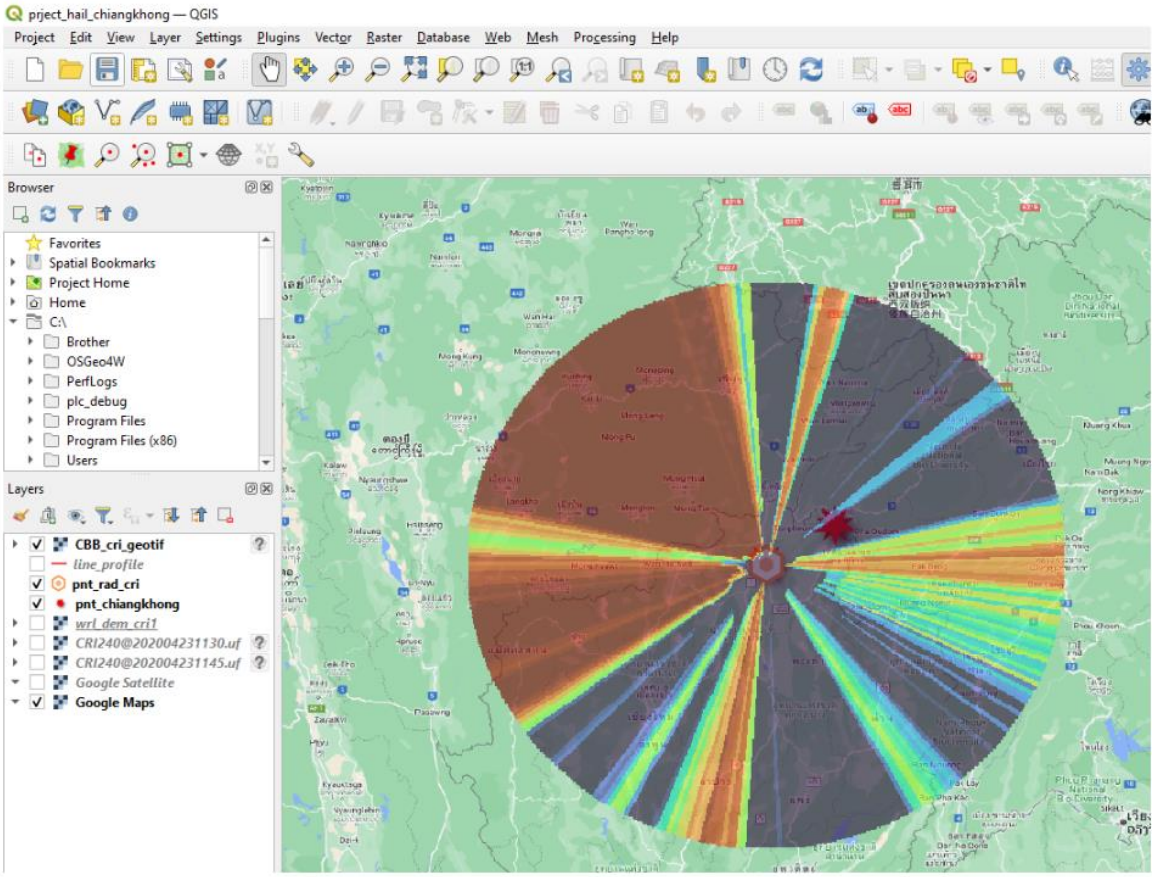

Figure 7: CBB exported from Python using Wradlib functions, displayed in QGIS overlaid on a base map for the Chiang Rai radar observation area

4.4 Analyze the second elevation angle

When the elevation angle is increased to 1.5 degrees, PBB pattern shows notable changes compared to the lower elevation as shown in Figure 8. Significant blockage areas persist in the western and northwestern sectors of the radar's observation range, as evident in the Beam-Blockage Fraction image. However, the eastern and southern regions experience substantially reduced blockage, offering clearer radar coverage in these directions. The improved visibility in the east and south has important implications for meteorological observations. It suggests that data from the Chiang Rai radar at this elevation angle can be reliably used to monitor various weather phenomena, including tropical storms and thunderstorms. Additionally, the clearer view enhances the radar's capability for aviation surveillance.

The analysis of radar beam blockage at multiple elevation angles provides crucial insights into the quality and limitations of radar observations. By quantifying these effects, we can

develop more effective strategies for radar scanning. This information is particularly valuable for organizations like TMD in optimizing their radar operations and data utilization policies. Understanding the spatial variations in beam blockage allows for targeted improvements in radar coverage and more accurate interpretation of radar data across different sectors and elevation angles.

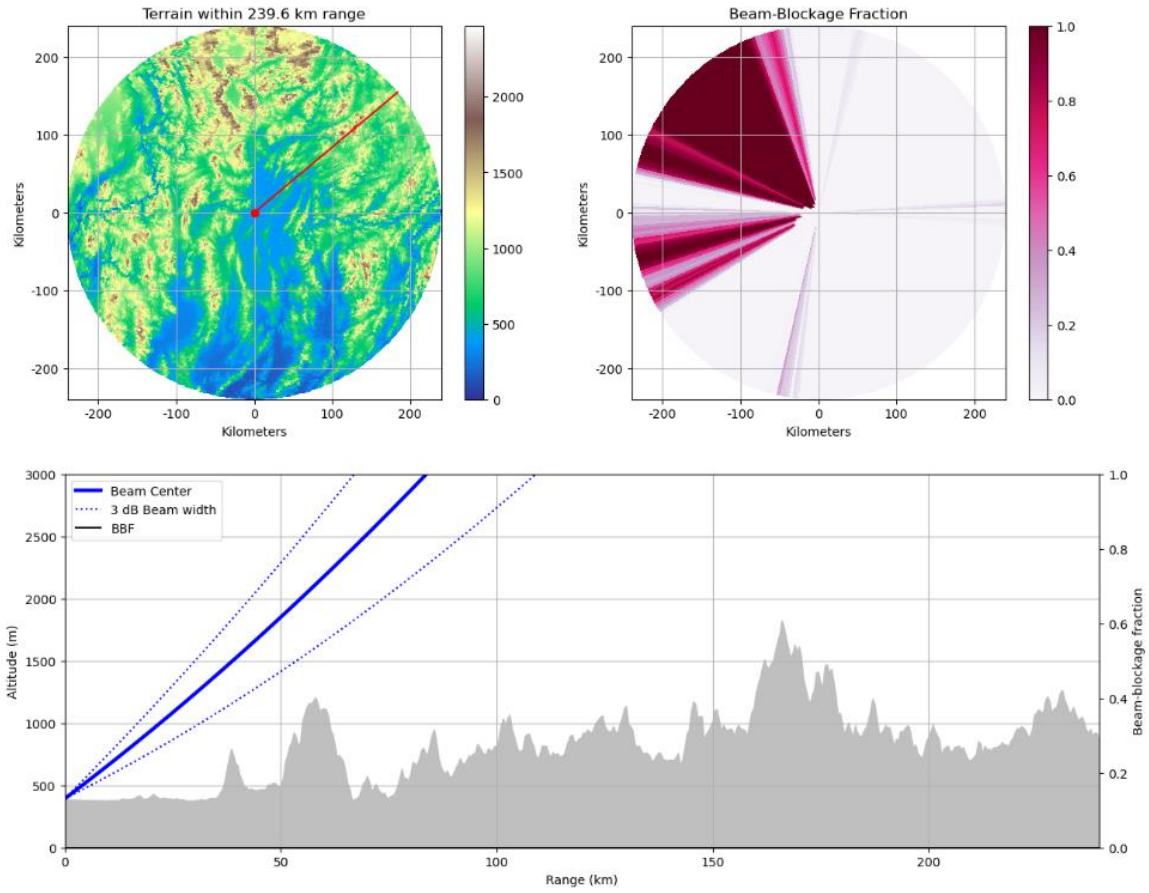

Figure 8: Results of beam simulation interacting with DEM for the second elevation angle of 1.5 degree

5. Discussion

PBB analysis for the Chiang Rai radar reveals significant spatial variability in beam obstruction, predominantly influenced by the complex topography of the region. The results demonstrate severe blockage (CBB > 0.8) in the western and northwestern quadrants, contrasting with minimal blockage (CBB < 0.2) in the eastern and southeastern sectors. This pattern aligns with the findings of Bech et al. (2003), who observed similar topography-induced blockage patterns in their study of weather radars in mountainous terrain. The interpolation of CBB data from polar to Cartesian coordinates, using both linear and nearest neighbor methods, provides a robust representation of the blockage patterns. This approach is consistent with the methodology proposed by Zhang et al. (2013), who emphasized the importance of accurate spatial representation of beam blockage for improved radar data quality.

The integration of CBB data into GIS through the creation of a GeoTIFF file marks a significant advancement in the visualization and analysis of radar beam blockage. This approach allows for precise correlation of blockage patterns with topographical features, urban areas, and other geographical elements, similar to the GIS-based analysis conducted by Kucera et al. (2004) in their study of radar coverage optimization. The observed reduction in beam blockage at higher elevation angles (1.5 degrees) in certain sectors, particularly in the east and south, has important implications for meteorological observations. This finding supports the work of Germann et al. (2006), who demonstrated the benefits of multi-elevation analysis in mitigating the effects of beam blockage on radar measurements. The persistent blockage in western and northwestern sectors, even at higher elevations, underscores the challenges posed by extreme topography, a phenomenon also noted by Krajewski et al. (2006) in their comprehensive study of radar-rainfall estimation in complex terrain.

The results of this study contribute to the growing body of knowledge on radar beam propagation in complex environments. The detailed analysis of beam blockage at multiple elevation angles provides crucial insights for optimizing radar operations, aligning with the recommendations of Manz et al. (2016) for improving weather radar networks in mountainous regions. The potential for enhanced monitoring of various weather phenomena, including tropical storms and thunderstorms, in less obstructed sectors at higher elevations, echoes the findings of Delrieu et al. (1995), who highlighted the importance of adaptive scanning strategies in areas with PBB. Furthermore, the implications for aviation surveillance in clearer sectors align with the work of Cho et al. (2017), emphasizing the multifaceted applications of weather radar data beyond traditional meteorological uses.

The methodology developed in this study, combining high-resolution terrain data with advanced radar simulation techniques and GIS integration, offers a comprehensive approach to quantifying and visualizing beam blockage. This general method addresses the limitations noted by Gabella and Perona (1998) in earlier beam blockage studies, providing a more accurate representation of the spatial variability in radar coverage. The potential for using this information to develop targeted improvements in radar coverage and data interpretation strategies is particularly significant for organizations like TMD. This application of beam blockage analysis for operational optimization can be used to enhance the quality and utility of weather radar networks in diverse geographical sites.

6. Conclusion

Partial Beam Blockage (PBB) for the Chiang Rai weather radar revealed the complex interplay between radar beam propagation and northern Thailand's mountainous topography. In our investigation, beam obstruction varied spatially, with severe blockage (CBB > 0.8) in western and northwestern parts and low blockage (CBB < 0.2) in eastern and southeastern parts. This pattern matches the region's topography, demonstrating how geography affects radar data quality. The integration of high-resolution DEM with modern radar modeling techniques and the transfer of CBB data from polar to Cartesian coordinates have improved beam blockage pattern knowledge. The differences between linear and nearest neighbor interpolation approaches in trend continuity and data value preservation offer useful insights into data representation. The investigation at several elevation angles, especially 1.0 and 1.5

degrees, shows radar operation optimization potential. The lessened blockage in eastern and southern sectors at higher elevations reflects improved tropical storm and thunderstorm monitoring and aircraft surveillance. QGIS visualization shows that CBB data may be integrated into GIS platforms to correlate beam blockage patterns with topographical and urban factors. This integration confirms our data processing technology and provides a powerful radar coverage spatial analysis tool. These findings affect radar meteorology, especially in challenging environments. This process can assist organizations such the Thai Meteorological Department to optimize radar operations, improve data interpretation, and improve regional weather forecasting and monitoring.

References:

Bech, J., Codina, B., Lorente, J., & Bebbington, D. (2003). The sensitivity of single polarization weather radar beam blockage correction to variability in the vertical refractivity gradient. Journal of Atmospheric and Oceanic Technology, 20(6), 845-855. https://doi.org/10.1175/1520-0426(2003)20<845:TSOSPW>2.0.CO;2

Gou, Y., & Chen, H. (2021). Combining Radar Attenuation and Partial Beam Blockage Corrections for Improved Quantitative Application. Journal of Hydrometeorology, 22(1), 139-153. https://doi.org/10.1175/JHM-D-20-0121.1

Cho, J. Y. N., Newell, R. E., Anderson, B. E., Barrick, J. D., & Thornhill, K. L. (2017). Characterizations of tropospheric turbulence and stability layers from aircraft observations. Journal of Geophysical Research: Atmospheres, 122(6), 3448-3465.

Dai, Q., Yang, Q., Han, D., Rico-Ramirez, M. A., & Zhang, S. (2019). Adjustment of radar-gauge rainfall discrepancy due to raindrop drift and evaporation using the Weather Research and Forecasting model and dual-polarization radar. Water Resources Research, 55(11), 9211-9233. https://doi.org/10.1029/2019WR025517

Delrieu, G., Creutin, J. D., & Andrieu, H. (1995). Simulation of radar mountain returns using a digitized terrain model. Journal of Atmospheric and Oceanic Technology, 12(5), 1038-1049.

Friedrich, K., Kalina, E. A., Aikins, J., Gochis, D., & Rasmussen, R. (2016). Precipitation and cloud structures of intense rain during the 2013 Great Colorado Flood. Journal of Hydrometeorology, 17(1), 27-52. https://doi.org/10.1175/JHM-D-14-0157.1

Gabella, M., & Perona, G. (1998). Simulation of the orographic influence on weather radar using a geometric-optics approach. Journal of Atmospheric and Oceanic Technology, 15(6), 1485-1494.

Germann, U., Galli, G., Boscacci, M., & Bolliger, M. (2006). Radar precipitation measurement in a mountainous region. Quarterly Journal of the Royal Meteorological Society, 132(618), 1669-1692.

Heistermann, M., Jacobi, S., & Pfaff, T. (2013). Technical Note: An open source library for processing weather radar data (wradlib). Hydrology and Earth System Sciences, 17, 863–871. https://doi.org/10.5194/hess-17-863-2013

Krajewski, W. F., Vignal, B., Seo, B. C., & Villarini, G. (2006). Statistical model of the range-dependent error in radar-rainfall estimates due to the vertical profile of reflectivity. Journal of Hydrology, 328(1-2), 83-97.

Kucera, P. A., Krajewski, W. F., & Young, C. B. (2004). Radar beam occultation studies using GIS and DEM technology: An example study of Guam. Journal of Atmospheric and Oceanic Technology, 21(7), 995-1006.

Mahavik, N., Tantanee, S., & Masthawee, F. (2023). Dual-Polarimetric Radar Applications for Investigating Severe Thunderstorms in Northern Thailand during the Pre-

Monsoon Season. Applied Environmental Research, 45(4). https://doi.org/10.35762/AER.2023026

Mahavik, N., Tantanee, S., & Masthawee, F. (2024). Spatial assessment of produced hailstorm maps in severely affected areas in Northern Thailand based on dual-polarimetric radar using the cloud computing platform Google Earth Engine. Applied Geomatics. https://doi.org/10.1007/s12518-024-00569-4

Manz, B., Buytaert, W., Zulkafli, Z., Lavado, W., Willems, B., Robles, L. A., & Rodríguez-Sánchez, J. P. (2016). High-resolution satellite-gauge merged precipitation climatologies of the Tropical Andes. Journal of Geophysical Research: Atmospheres, 121(3), 1190-1207.

McKee, J. L., & Binns, A. D. (2016). A review of gauge–radar merging methods for quantitative precipitation estimation in hydrology. Canadian Water Resources Journal, 41(1-2), 186-203. https://doi.org/10.1080/07011784.2015.1064786

Saltikoff, E., Cho, J. Y. N., Tristant, P., Huuskonen, A., Allmon, L., Cook, R., Becker, E., & Joe, P. (2016). The Threat to Weather Radars by Wireless Technology. Bulletin of the American Meteorological Society, 97(7), 1159-1167. https://doi.org/10.1175/BAMS-D-15-00048.1

Saltikoff, E., Haase, G., Delobbe, L., Gaussiat, N., Martet, M., Idziorek, D., Leijnse, H., Novák, P., Lukach, M., & Stephan, K. (2019). OPERA the Radar Project. Atmosphere, 10(6), 320. https://doi.org/10.3390/atmos10060320

Speirs, P., Gabella, M., & Berne, A. (2017). A comparison between the GPM dual-frequency precipitation radar and ground-based radar precipitation rate estimates in the Swiss Alps and Plateau. Journal of Hydrometeorology, 18(5), 1247-1269. https://doi.org/10.1175/JHM-D-16-0085.1

Zhang, P., Zrnic, D., & Ryzhkov, A. (2013). Partial beam blockage correction using polarimetric radar measurements. Journal of Atmospheric and Oceanic Technology, 30(5), 861-872. https://doi.org/10.1175/JTECH-D-12-00075.1